ORIGINAL ARTICLE

Dissimilar material joining of densified superwood to aluminum by adhesive bonding

Matt Hartsfield[1] · Bo Chen[2] · Yu Liu[3] · Shuaiming He[3] · Ulrich H. Leiste[4] · William L. Fourney[2,4] · Teng Li[2] · Liangbing Hu[3] · Alan A. Luo[1,5]

Abstract

Superwood is a densified wood product that shows promise as a lightweight and renewable alternative for metallic materials. In order for this high-performance new material to be used in multi-material products, it must be able to be joined with other major materials. For example, joining superwood to aluminum would provide a key enabling technology for its use in automotive components since aluminum is presently a major lightweight material for such applications. In this paper, a methacrylate-based adhesive has been identified to provide high lap shear strength (7.5 MPa) for aluminum-to-superwood joints. The aluminum-to-superwood samples were prepared with different amounts of pre-polishing to create openings to the pores in the superwood so adhesive could penetrate into them and create a mechanical interlock, in addition to the hydrogen/chemical bonding at the surface between the methyl methacrylate (MMA) in methacrylate-based adhesive and the cellulose in superwood. For aluminum samples, a thin layer (typically a few nanometers) of oxide film on the surfaces provides hydrogen/chemical bond to MMA structure in the adhesive layer. The failure strength of the superwood-to-aluminum joint sample is about 50% higher than that of natural wood to natural wood joint sample and comparable to that of aluminum-to-aluminum joint sample.

1 Introduction

Superwood is a lightweight and high-performance material created by chemically treating natural wood to partially remove lignin and then compressing the treated wood into a much denser material [1]. This creates a significantly stronger structural material than natural wood while remaining a renewable resource. This novel material is very lightweight, being about half the density of Al 5754, with twice the ultimate tensile strength. An important step in bringing this material to an application stage is to develop technology and best practices for joining superwood to other common structural materials such as aluminum alloys. To fully exploit the excellent properties of the superwood material, advanced joining techniques must be developed for applications.

Mechanical joining is the simplest method of joining wood to metal, as it does not require much alteration from metal-to-metal joining, but it has several drawbacks such as only forming joints at discrete intervals, creating stress concentrations, or requiring certain moisture contents [2, 3]. Stir welding has successfully been used to join aluminum to wood but has the drawback of using an interfacial material to aid in joining [4] as well as being dependent on the fiber angle of the wood [5]. Chemical joining such as adhesives can mitigate some of these issues. Adhesives do have some

Matt Hartsfield, Bo Chen, and Yu Liu contributed equally to this paper.

✉ Alan A. Luo
luo.445@osu.edu

1 Department of Materials Science and Engineering, The Ohio State University, Columbus, OH 43210, USA

2 Department of Mechanical Engineering, University of Maryland, College Park, MD 20742, USA

3 Department of Materials Science and Engineering, University of Maryland, College Park, MD 20742, USA

4 Department of Aerospace Engineering, University of Maryland, College Park, MD 20742, USA

5 Department of Integrated Systems Engineering, The Ohio State University, Columbus, OH 43210, USA

pretreatment requirements depending on the adhesive and the materials ranging from simple cleaning of the surface to needing to prime it with a second compound [6]. Many types of pretreatment have been extensively tested for metals such as aluminum [7, 8]. The problem with adhesives is that, unlike many mechanical fasteners, the adhesive will not always bond to different materials with the same strength.

While superwood is an altered form of wood, it maintains similar structural makeup to natural wood, the main difference being the collapse of pores during densification. These pores are used when creating a strong adhesive bond with natural wood substrates, with adhesive moving through the pores to penetrate deeper within the material [9]. It is important to improve the quality of the surface for adhesive bonding to mitigate the reduction in pores during densification. In natural wood, it has been shown that the wettability of the surface has a strong correlation to the bond strength and is easily increased by abrading the surface [10]. This also has the effect of removing surface contaminants that could interfere with the bonding [11]. Care must be taken to avoid crushing and burnishing the surface when abrading, as this causes the natural wood surface to have significantly reduced wettability and bond strength [12]. The surface roughness of natural wood can be correlated to an increase in adhesion strength [13]. The precise roughness of the surface is difficult to predict. The roughness is dependent on the pre-processing structure of natural wood as it creates irregularities in the surface not due to any surface treatment, causing surface roughness comparisons between samples to be highly variable [14]. Moisture content must be monitored, as excess moisture can cause thinning of the adhesive at the interface, while overly dry wood can resist wetting from the adhesive, preventing adhesive penetration [9]. Less research has been done on the interface between natural wood and adhesive and its failure mechanism. What has been performed shows that failure is partially caused by the cell wall swelling at the surface, which is dependent on both moisture content and whether the sample is old or new wood, referring to growth stages in natural wood, as the cellular structure between the two differs [15].

The goal of this research is to develop adhesive bonding technology for superwood, especially for dissimilar material joints to metallic materials for structural applications. One such application is the automotive industry, where adhesives are commonly used in joining dissimilar materials [16] Adhesives are used both to create the joint, as well as reduce galvanic corrosion seen when dissimilar metals are in physical contact [17]. Superwood is desirable in structural applications as it is created from wood, which is a renewable resource and the increase in the material strength also should lead to an increase in joint strength [18]. The trees used to create superwood take in CO_2 and provide fresh oxygen making them desirable when structural manufacturers are looking to reduce their carbon footprint and work towards a green future. The trees are limited in the size they can grow to so joining techniques are needed to join superwood to itself and other materials. The use of these joints in application has led to rigorous testing methods for adhesive joining, notably as used here, lap shear testing [19].

Figure 1 is a schematic showing the proposed bonding mechanisms between aluminum and the superwood in this investigation. The methacrylate adhesive was selected because the MMA polymer bonds to the aluminum and its surface oxides through hydrogen bonding and carboxylate ionic bonding [20]. It also adheres to the cellulose and lignin in the superwood substrate by hydrogen/chemical bonding and through penetrating the pores to create a mechanical interlock [21]. The joining process development and failure mechanism discussions in this investigation are based on the bonding mechanisms depicted in Fig. 1.

2 Experimental procedures

2.1 Material selection and preparation

Superwood was prepared by a two-step process described by Song et al. [1]. This material was cut into 25.4-mm-wide by 101.6-mm-long strips, with the width being measured in the direction transverse to the fiber direction and the length being measured along the fiber direction. These samples were on average 2.7 mm thick before any surface preparation, with ranges from 2.5 to 2.9 mm due to slight differences
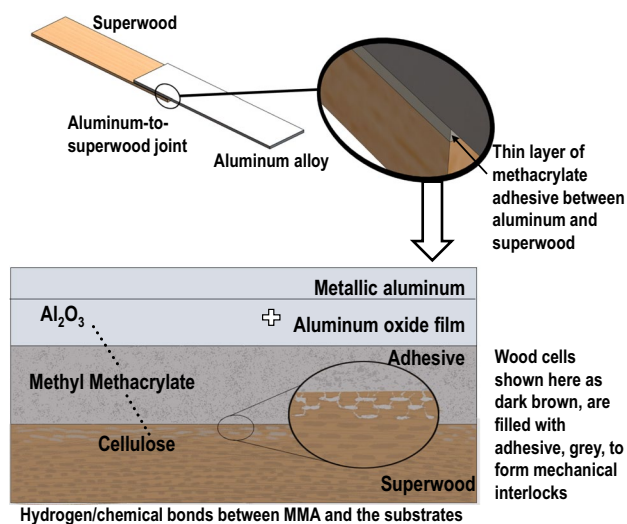

Fig. 1 Adhesive joining between superwood and aluminum. The lap shear joint is made of superwood and aluminum with a 25.4 mm by 25.4 mm overlap area where the adhesive is applied. The methacrylate adhesive adheres to the cellulose and lignin in the superwood through hydrogen/chemical bonding while penetrating into pores in the superwood to create a mechanical interlock

between batches. Samples of the same width and length were cut from 2-mm-thick Al5754 with a nominal composition of Al-3.1 Mg-0.4Mn (all in weight percentage). This alloy was chosen due to its common use in the automotive industry. The joint sample dimensions, as shown in Fig. 2, followed ASTM D1002 and D5868, the standards for single lap shear testing of metal and fiber-reinforced plastic, respectively.

The adhesive used in the first set of samples was Plexus MA832, a methacrylate adhesive designed to adhere to metal without primers. The adhesive was chosen due to its application in the automotive industry specifically with non-metal substrates such as fiber-reinforced polymer composites. Its ability to bond well with non-metal substrates suggested

that it would likely bond better with superwood than adhesives designed only for joining metals. The methacrylate also had the benefit of being time cured rather than heat cured, as studies in natural wood have shown that density and mechanical properties change in wood after heat treatment which could negatively affect the joint [22]. Other adhesives were considered and discarded as unsuitable. A primary consideration was to use adhesives currently used as structural adhesives in the automotive industry to bond metals to non-metallic substrates. Several epoxies are specifically designed for wood to metal bonding, but none is used as structural adhesives in the auto industry. Several adhesives that are used in the automobile industry for wood to
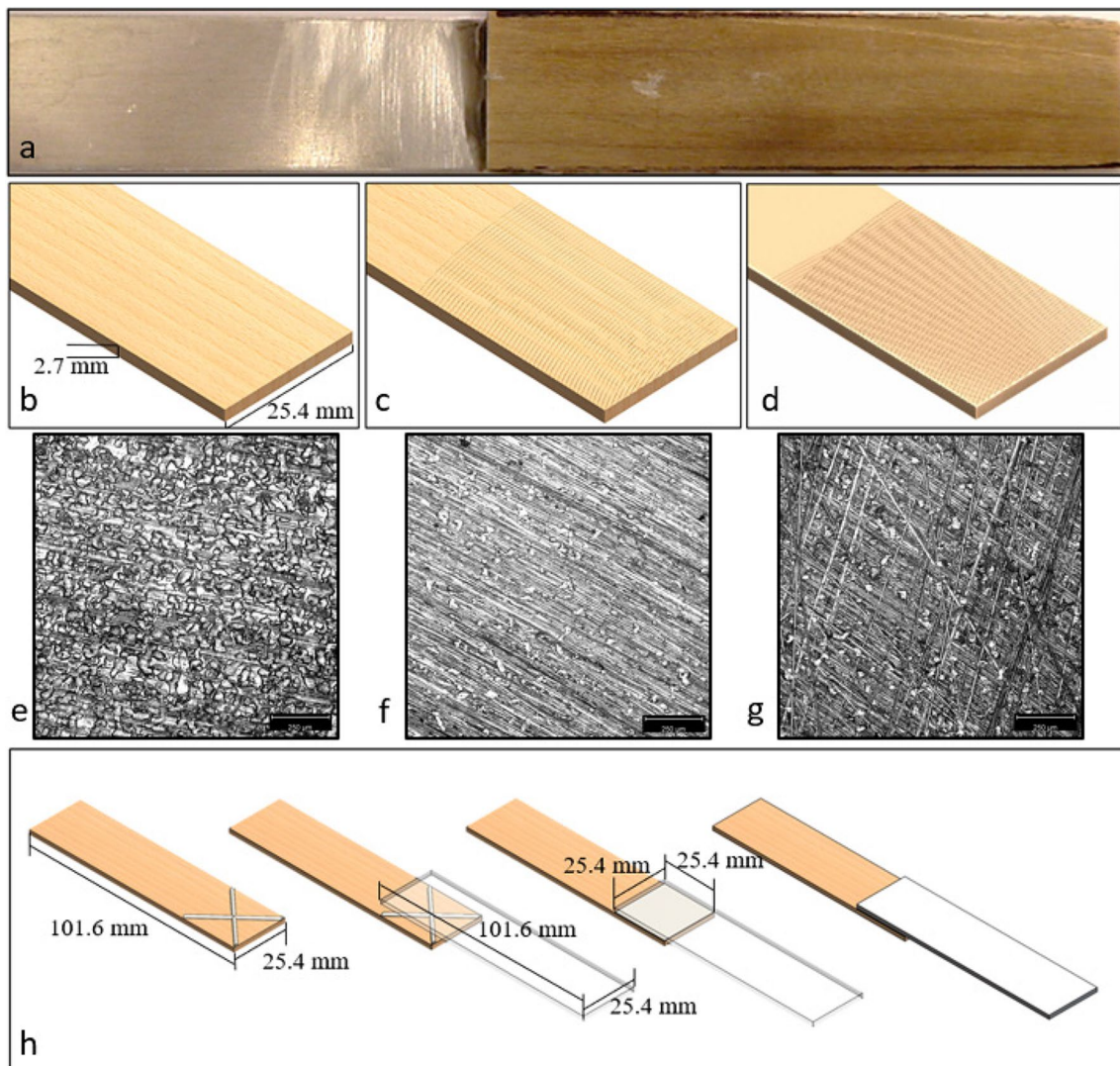

Fig. 2 Joint design. **a** Assembled joint. **b** No surface preparation (NS) superwood model. **c** Oriented polishing superwood model with polishing all oriented transverse to the fiber direction (OS). **d** Randomly oriented polishing model (RS). **e** Optical microscopy of NS sample, all optical microscopy at ×10 magnification, scale equals 250 μm. **f** Optical microscopy of OS sample. **g** Optical microscopy of RS sample. **h** Adhesive application. The adhesive is applied in an x-pattern to one substrate, and then, the other substrate is placed on top of the adhesive and pressed to spread the adhesive across the entire surface area of the joint

non-metal bonding were evaluated, but initial testing showed inferior performance to the Plexus MA832 used in this study.

2.2 Adhesive sample preparation methods

All samples had adhesive applied in an x-pattern to the aluminum in the 25.4 mm overlap area to guarantee the even spread of the adhesive across the entire bonding area as seen in Fig. 2e. Glass bead spacers of 254-micron diameter were added to the adhesive to ensure a consistent layer height. The superwood was placed over the adhesive, and pressure was applied to spread the adhesive across the area, with adhesive overflow being removed before the samples were left to cure at room temperature and ambient humidity, approximately 20 °C and 42% humidity, for 24 h.

Surface preparations included no surface preparation (designated as NS) to create a baseline value for the adhesive on raw material, shown in Fig. 2b, sanding of both aluminum and superwood with 320 grit sandpaper with scratches oriented in the same direction transverse to the fiber direction (designated as OS) seen in Fig. 2c, and sanding with the scratches randomly oriented (designated as RS), shown in Fig. 2d. Using the GX53 Olympus optical microscope and the plugin SurfCharJ developed by Chinga et al. [23] for ImageJ [24] to evaluate the three surface preparation methods on the aluminum samples, similar arithmetical mean deviation (Ra) values were found. NS had an Ra of 54.6 μm, OS had an Ra of 46.6 μm, and RS displayed an Ra of 45.8 μm. As expected, the OS and RS samples have nearly identical surface roughness as they were treated with the same sandpaper, differing only in scratch direction.

The samples also underwent three different pressing forces during curing: 0 N, 667 N, and 1334 N. These forces were applied using one-handed bar clamps through the entire curing process, using the maximum force of the clamp. The only force applied to the 0 N samples was the force of manually holding the top and bottom sheet together when assembling samples. In addition, tests were done using a vice and hammer to create indentations on the material surface. One sample set was made using the indentations solely on the aluminum sheet, and one set was made using the indentations on both the aluminum and the superwood. These allowed for testing of a different pattern of surface roughness than scratches.

2.3 Testing procedures

The single lap shear specimens were tested in tension using an MTS Criterion Model 43 with a crosshead speed of 2 mm/min. This lies between the speeds dictated by the two ASTM standards for lap shear referenced, with D1002 using a speed of 1.3 mm/min and D5868 using a speed of 13 mm/min. Offsets were used in the grips to center the joint in the machine and avoid out-of-plane stresses. To mitigate the eccentric loading seen in single lap shear due to the offsets, double lap shear specimens were made to match the RS1334 sample preparation to show comparable results between the two tests. Joint strength was measured by dividing the average load of failure by the adhesive area of the joint, 645.16 mm^2. All samples used the same adhesive area.

2.4 Characterization

The microstructure of the superwood and natural wood was characterized by using a Hitachi SU-70 Schottky field-emission gun scanning electron microscope (SEM) (2–5 kV). The SEM samples are processed by gold sputtering before the test. Basswood was selected as the starting material, which is a kind of hardwood. Natural wood contains many lumina (tubular channels 15–80 μm in diameter) along the wood growth direction (Fig. 3a–c). The larger lumen diameters (30–80 μm) are vessels, whereas the smaller diameter (approximately 15–35 μm) lumens are cellulose fibers. By partial removal of lignin/hemicellulose from the wood cell walls, followed by hot pressing, the wood lumina as well as the porous wood cell walls collapse entirely, resulting in a densified piece of about 3 times the density of natural wood (from 0.42 to 1.3 g/cm^3) (Fig. 3d). The superwood has a unique microstructure: the fully collapsed wood cell walls are tightly intertwined along their cross-section (Fig. 3e) and densely packed along their length direction (Fig. 3f), which has strengthened the intermolecular interactions between cellulose molecules. The strong interaction among cellulose fibers will enhance the joint strength of superwood to other materials such as aluminum.

3 Results

3.1 Joint strength

Figure 4 shows the maximum joint strength of aluminum-to-superwood (7.6 MPa) achieved in this investigation, in comparison with the maximum strengths reported in literature for aluminum-to-aluminum [25–27] and natural wood-to-wood [28] joints and to tests done on superwood-to-superwood bonding of samples using the same adhesive as the superwood-to-aluminum. The adhesive joint strength of natural wood was between 2 and 5 MPa depending on surface roughness, with surface roughness of 1.2 to 1.7 μm producing the best results [25]. These tests were done using single strap testing, with a larger bonding area of 2425 mm^2, compared to the single lap shear 645.16 mm^2. An epoxy resin was used in these samples with similar shear strength (16.6 MPa when using aluminum as substrate as per manufacturer data sheets) to the MMA adhesive used in superwood bonding (13.8–19.3
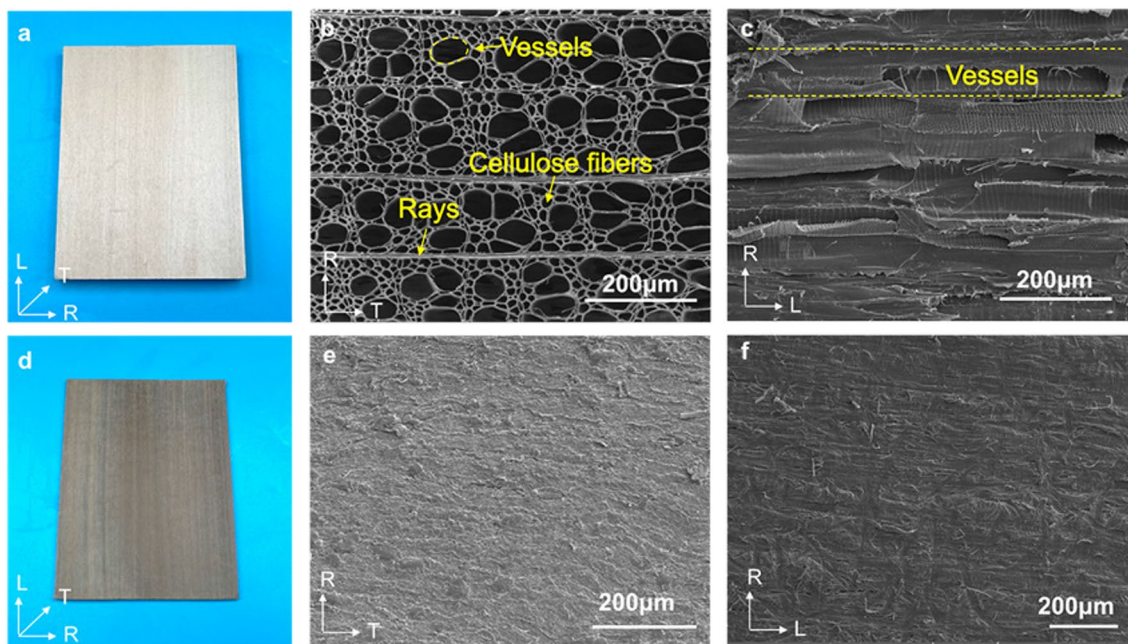
Fig. 3 **a** Photograph of natural wood sample. **b** SEM image of the natural wood sample in the RT plane. **c** SEM image of the natural wood sample in the RL plane, revealing the cross-section view of the lumina along the L direction. **d** Photograph of superwood. **e** SEM image of the densified wood in the RT plane, showing the fully collapsed lumina. **f** SEM image of the densified wood in the RL plane shows the dense laminated structure
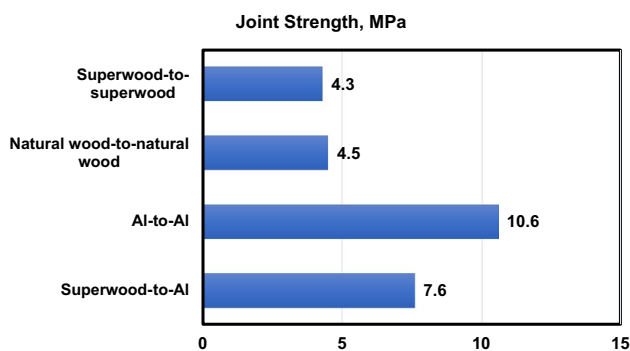

Fig. 4 Maximum joint strength of aluminum-to-superwood joints achieved in this study, compared to aluminum-to-aluminum, natural wood-to-wood, and superwood-to-superwood joint strengths. Note: differences in adhesive. Superwood-to-Al, natural wood-to-natural wood, and superwood-to-superwood all have adhesives with average shear strength of 16.5 MPa. Al to Al has adhesive with average shear strength of 23.4 MPa

MPa as per manufacturer data sheets). In aluminum bonding with Plexus MA 300 poly methyl methacrylate (PMMA) adhesive, Maćkowiak et al. [28] saw that with the stronger MA300 methacrylate adhesive (20.7–26.2 MPa shear strength as per manufacturer data sheet), there was a butt-joint yield stress of 21.2 MPa. Using the Tresca uniaxial shear stress failure theory, this joint can be approximated to have a 10.6 MPa shear stress. This estimates a shear stress of 45.2% of the listed

strength. Applying this to the stress given in the manufacturer data sheet for Plexus MA832 would predict a strength of 7.5 MPa, with experimental data giving a strength of 7.61 MPa in aluminum to superwood joints. The superwood-to-superwood joint showed failure at 4.3 MPa due to poor penetration of adhesive into the superwood materials due to reduced pore sizes (collapsed cells as shown in Fig. 3e) in the microstructure. The aluminum-to-superwood joints in this study provide significantly higher (about 50% higher) strength (7.61 ± 1.1) than natural wood-to-wood (4.50 ± 0.25) and superwood-to-superwood (4.26 ± 2.0) joints and comparable strength to aluminum-to-aluminum joints (10.9 ± 0.7) given the increase in adhesive strength in the aluminum-to-aluminum literature.

3.2 Failure modes

Failure surfaces in wood, both natural and superwood samples, can be difficult to characterize as failures in the adhesive versus failures in the wood. ASTM D5266-99 defines shallow and deep wood failure and provides methods for estimating the percentage of wood failure in adhesively bonded wood joints. Shallow wood failure occurs in the top 1–2 layers of cells beneath the adhesive layer, and the fracture path is unaffected by the grain structure within the wood. This type of failure is undesirable in lap shear joints, as this leads to failure at low loads.
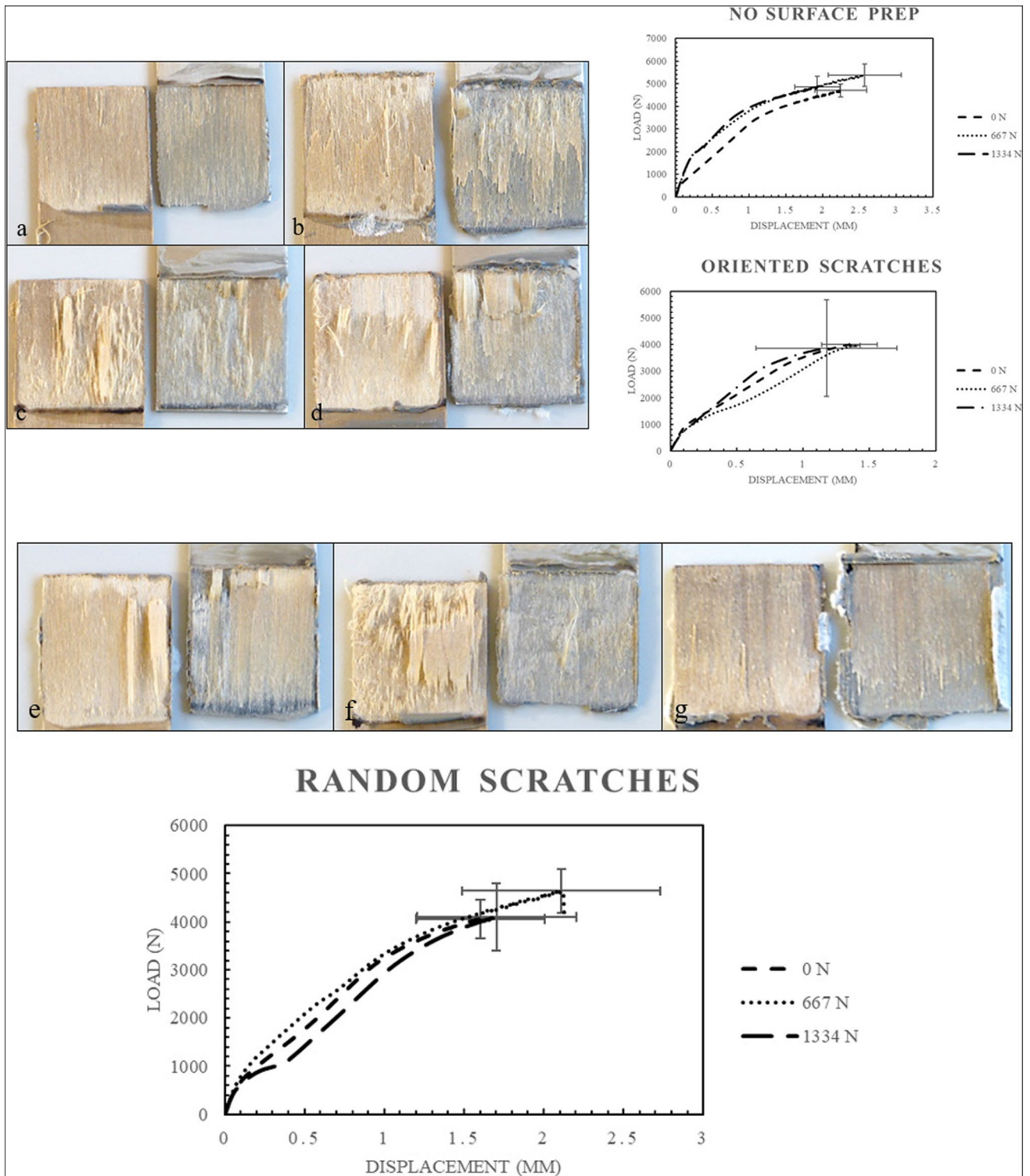
Fig. 5 Failure surfaces and stress-displacement curves of **a** no surface treatment 0 N, **b** no surface treatment 1334 N, **c** oriented scratches 0 N, **d** oriented scratches 1334 N, and **e** random scratches 0 N. **f** Failure surface and stress-displacement curve of random scratches at 667N. **g** Failure surface and stress-displacement curve of random scratches at 1334 N

Figure 5 shows the joint strength and failure surfaces of aluminum-to-superwood samples prepared in different conditions, with an average stress at failure ranging from 5.98 to 7.75 MPa. Polishing the superwood surface to have oriented scratches transverse to the fiber direction caused the superwood to have a less uniform failure surface. Portions of

the failure surface show that the scratches open the cells and allow adhesive to penetrate deeper and create deeper failure, but portions of the failure surface are shallow failure as seen in the untreated superwood. The samples with randomly oriented scratches that experienced no pressure during curing show similar fracture patterns to the oriented scratch samples with 667 N applied pressure. This may imply that the randomized scratches allow for further penetration into the superwood of the adhesive similar to what a low applied pressure does. The full list of the failure loads, extensions, and stresses at different surface preparations and curing forces can be seen in Table 1.

Deep wood failure as per the ASTM standard occurs further in the wood than shallow wood failure and exhibits fracture paths strongly influenced by the grain angle and growth rings of the wood. Large portions of deep failure are seen beginning with the randomly oriented scratch samples that underwent 667 N pressure during curing. These samples showed thicker sections of the superwood surface torn during failure, as well as some gentle curving of the failure surface edges along the grain boundaries. This implies a failure following the grain boundaries as is characteristic of deep wood failure. The grains in the transverse direction are aligned with the fiber growth, making failure in the transverse direction difficult to characterize as following the grains rather than failing in a manner unaffected by grain structure as in shallow failure, so in transverse failure depth is the best way to characterize the deep failure. These samples failed at 4640 N of load and 2.11 mm of extension, outperforming all samples but the samples with no surface treatment and no pressure.

The 1334 N random orientation samples show the deepest failure out of the tested pressure and surface preparation combinations and the clearest indications of influence from the grain in the fracture surface. The sample shown has some slight color variation between the grains near the center of the fracture surface, and the failure is deep enough that same color variation can be clearly seen in the superwood that remains attached to the adhesive on the aluminum substrate. These samples fail at 4906 N and 2.06 mm of extension on average, the highest force and third highest extension.

Double lap shear samples were tested to determine any effects the eccentric loading present in single lap shear had on the failure load and displacement. The samples were made with randomly oriented scratches and 1334 N of clamping force with 2 pieces of the 101.6×25.4×2 mm Al 5754 being adhered between two pieces of 50.8×25.4×2.7 mm superwood. The samples had the same total adhesive area as the single lap shear samples, allowing for direct comparison of the two tests. The failure surface continued to show deep wood failure as was seen in the single lap shear samples, but the double lap shear had more consistency in failure load and extension than the single lap shear. This is due to the removal of the eccentric loads. These samples had significantly less variation in the maximum load and extension of the joints than single lap shear, as well as having a defined elastic region. This more clearly shows the change in the slope of the load–displacement curve as the fibers of the superwood begin to separate from the bulk of the material under the shear load.

To further test how altering the substrate surface can affect the failure of the joint, superwood and aluminum were patterned using a vice and hammer to create patterned dents, shown in Fig. 6. The dents proved to excessively damage the superwood, becoming crack initiators, so instead the aluminum was patterned while the superwood was more roughly polished with 80 grit sandpaper. Glass bead spacers were not used in these tests.

These proved to greatly increase the adhesion of the joint. The joint failed in the superwood, leaving several even layers of superwood fibers on the adhesive after failure thick enough to completely obscure view of the adhesive. More superwood layers adhere to the adhesive leading to several layers of superwood peeling off from the

Table 1 Average and maximum failure loads, extensions, and strength of the samples at different preparations and clamping forces

| Sample prep	Clamping force	Avg failure extension (mm)	Avg failure load (N)	Max failure extension (mm)	Max failure load (N)	Avg strength (MPa)	Max strength (MPa)
No surface prep	0 N	2.24	4707.39	2.28	4967.85	7.2	7.7
	667 N	2.57	5384.21	2.97	5673.51	8.3	8.7
	1334 N	1.92	4860.6	2.06	5229.76	7.5	8.1
Oriented scratches	0 N	1.34	3968.85	1.64	3989.65	6.1	6.1
	667 N	1.33	3911.47	1.39	3954.48	6.0	6.1
	1334 N	1.17	3860.14	1.17	3860.14	5.9	5.9
Random scratches	0 N	1.6	4059.75	2.14	4425.09	6.2	6.8
	667 N	2.1	4640.5	2.98	5207.32	7.1	8.0
	1334 N	1.7	4096.41	2.06	4910.31	6.3	7.6
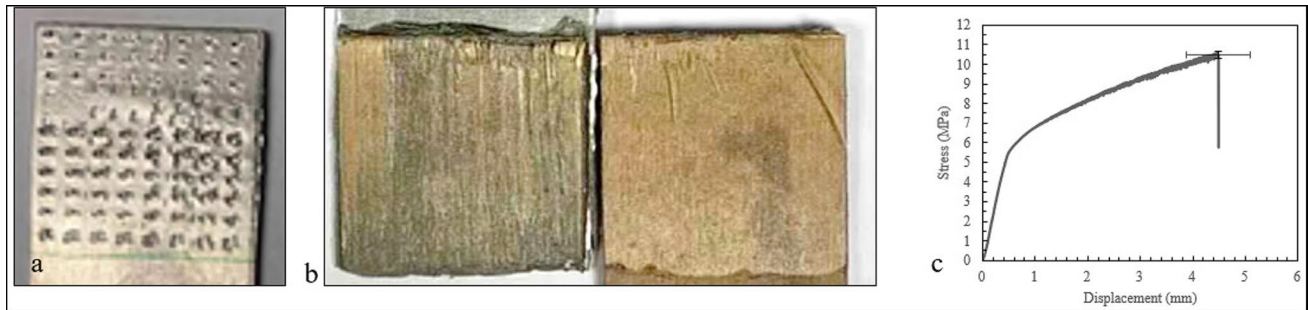
Fig. 6 **a** Aluminum patterned using vice and hammer. **b** Failure surface of sample with patterned aluminum and sanded superwood. **c** Load–displacement of patterned aluminum

bulk of the superwood sample. It also shows significant improvement in the failure load and extension at failure, with the load increasing from 4910 to 6775 N and extension increasing from 2.06 to 4.49 mm. These samples had significantly less variation in the maximum load and extension of the joints than single lap shear, as well as having a defined elastic region. This more clearly shows the change in the slope of the load–displacement curve as the fibers of the superwood begin to separate from the bulk of the material under the shear load.

3.3 Fracture analysis

Samples were studied under SEM to determine if there was information on the failure mechanism and adhesion that could be determined at that scale. Samples from the RS1334 group were tested, and imaging showed, in significantly

more detail, the damage to the superwood fibers at failure. Fibers that were attached to the adhesive were torn away from the bulk of the superwood as the sample was put under tension until the force was too strong and fibers broke seen in Fig. 7. Many of the individual fibers at the surface show breakage, though some remain in larger fiber bundles even after failure, retaining their structure despite the damage.

SEM was also used in determining the penetration of the adhesive into superwood, shown in Fig. 8. The adhesive was shown to charge up under the electron beam much quicker than the superwood, allowing for easier differentiation between the two materials which appear very similar under SEM as both are primarily carbon. Finding a portion of the cross-section taken with open vessels at the interface between the adhesive and superwood in a sample with random scratches and 1337 N clamping force, the adhesive can clearly be seen penetrated approximately 10 microns
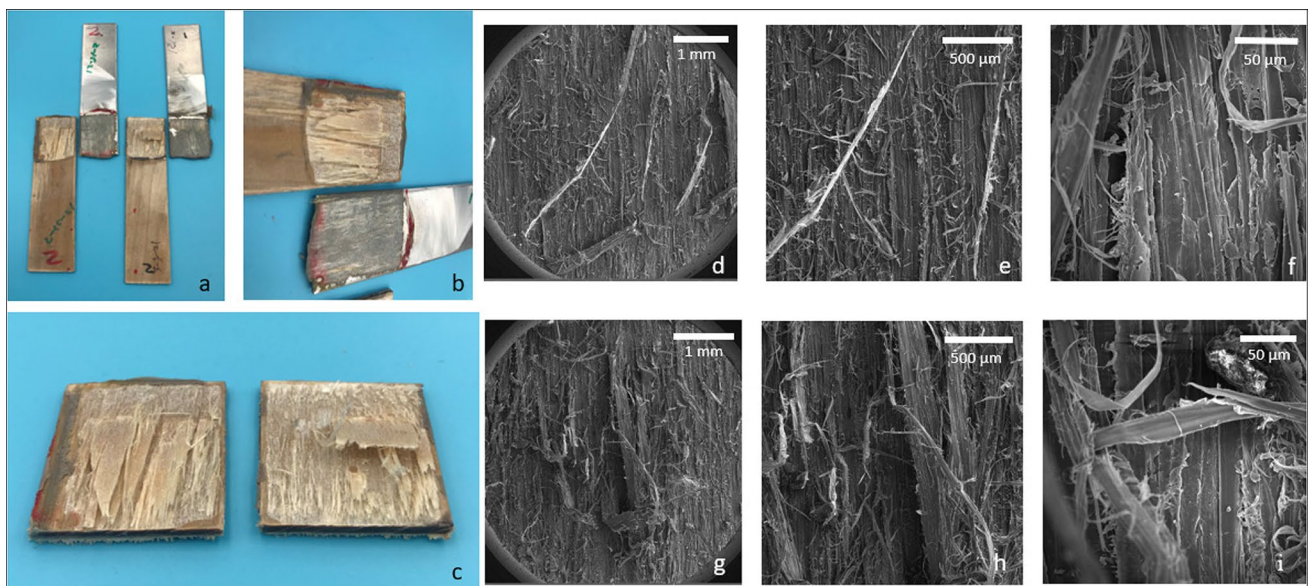

Fig. 7 **a** Photograph of two samples (RS1334) examined under SEM. **b** Closer image of left double sample on both aluminum and superwood sides of failure. **c** Cutoff failure surfaces for SEM imaging. **d**–**f** Left sample at various magnifications. **g**–**i** Right sample at various magnifications
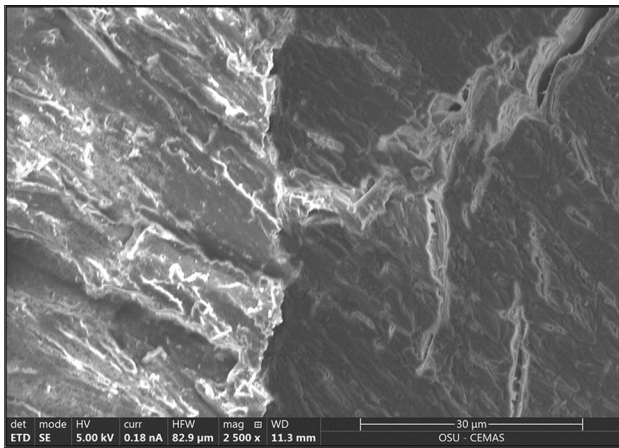
Fig. 8 SEM image of the adhesive-superwood interface. Superwood is on the right with adhesive on the left penetrating into the open vessel halfway down the image

into the open vessel in the superwood seen in Fig. 8. Due to relying on charge up to show clear differences between the two materials, samples are quickly made unusable as the superwood begins to charge up after a few minutes under beam, so SEM testing of adhesive penetration is limited.

4 Discussion

4.1 Bonding process parameters to joint strength

Among the average joint test curves, the 667 N clamping shows stronger mean results than the 0 and 1334 N samples of each preparation, with both higher elongation and failure load at failure as seen in Fig. 5. However, one of the 1334 N clamping samples had the highest failure load for an individual sample. This may imply that the best force to apply during curing is somewhere in between the two values. The 1334 N samples do have some low values that may be caused by more adhesive being forced out of the bond area than is truly in excess of the adhesive needed for bonding during the clamping. The 0 N samples tend to perform poorly in regard to depth of failure, showing scarce fiber covering of the adhesive surface and areas of adhesive with no wood visible of its surface, as some pressure is needed to force adhesive into the pores of the superwood. The samples with no surface preparation show the shallowest failure of all samples, with the superwood failing at the wood-adhesive interface. The samples show a fine layer of superwood fibers remaining on the adhesive at failure, while all other samples show some areas where the adhesive penetrated more deeply than the first layer of cells and the superwood fibers stay together. The oriented sanding samples showed a lower strength than those without surface treatment. In the no surface treatment

samples, there is some surface roughness due to the process of making superwood, which creates a shallow but random surface roughness. There is also a deeper roughness from the wood structure itself, with the fibers creating an uneven surface. The oriented scratches remove this random roughness in the surface, replacing it with shallow grooves oriented in one direction. This removes any surface damage that aided in adhesion, while not increasing surface roughness enough to have a strong effect, as well as risking burnishing that can smooth the surface. Figure 5a–e shows shallow wood failure, occurring near the surface of the superwood and showing fracture paths unaffected by the grain structure. The shallow wood failure here largely occurs as a thin coating of wood fiber similar to sawdust left on the aluminum side of the joint, seen most clearly in Fig. 5a, with some larger sections of wood staying intact, such as in Fig. 5e where two thin strips can be seen pulled from the surface of the superwood but still maintain structure. It also shows areas opposite those two strips where no wood can be seen at the adhesive surface, again showing shallow failure. This shallow failure is indicative of a weak bond between the adhesive and the wood surface as the adhesive fails to penetrate deeply into the superwood. The low penetration depth may not overly affect the joint strength as evidenced by the failure strength being similar between the random scratches and no preparation at higher curing clamping force, but leaves the joint more susceptible to weakness caused by any surface contamination or damage as the bond is more superficial than that at a deeper penetration.

The samples with no surface treatment and lower force show high failure loads as the adhesive has a clean surface to adhere to, with no stray fibers acting as debris in the joint. However, these samples show a poor failure mode, as described in Sect. 3.2, as the lack of surface preparation prevents deeper penetration into the superwood. The no surface treatment samples made at the highest force performed worse than the samples made at lower loads, as though there was a slight increase in failure load and there was a significant drop in extension at failure, as without surface treatment to open the pores the force spread the adhesive across the sample and out of the joint rather than pressing it into the open pores. The RS1334 did not have this issue as the randomly oriented scratches opened pores for the adhesive to flow into and the force ensured the adhesive flowed deeper into the superwood. The randomly oriented scratches can, however, cause a burnishing effect, lowering the wettability and adhesion of the joint. This is due to the wood fibers that have been torn being pushed together as the sanding process continues, creating a smooth surface rather than a rough one. Both Fig. 5f and g show deep wood failure, with (f) showing a fracture path likely influenced by the grain structure and (g) showing failure deep enough into the superwood that the surface of the adhesive is completely coated in

superwood fibers. This is most clearly seen in Fig. 5f where alongside the large section of wood that is removed from the superwood surface while maintain structural integrity on the superwood side of the joint, large fibers can be seen on the aluminum side, the largest of which is in the center of the joint. These fibers are more substantial than the shallow wood failure, where the surfaces resemble sawdust. In Fig. 5g, the wood surface does not have the same amount of wood partially removed from the superwood bulk, but the wood attached to the aluminum side of the joint is intact enough and thick enough an impression of the grain structure can be seen, most obvious in the darker band of material near the center if the joint. The deeper penetration into the surface allows for larger surface area for the adhesive to bond to as the adhesive spreads into the wood through any pores or vessels that were not completely collapsed during densification [29].

Using a vice and hammer creates a rough surface without smearing the wood fiber in a way that can cause burnishing, though the rough points are more distinct and can become stress concentrators. The largest drawback to using a vice and hammer is that using excessive force on the vice can cause the indentations to cause cracks rather than create roughness to improve adhesion, which cannot happen using sandpaper. Using a combination of methods can prove best. Using a rougher sandpaper on the superwood can help the adhesive penetrate into the deeper layers of the superwood, since the 80 grit sandpaper may introduce deeper scratches than the 320 grit sandpaper, while using a vice and hammer on the aluminum creates a rougher surface than just using sandpaper. Using this method shows great enhancement of both maximum load and maximum extension over just using sandpaper on the substrates.

The double lap shear samples show results similar to the single lap shear samples with the same preparations; the results fall into the same range of final loads and displacements. However, the double lap shear shows the stiffness and work to failure more visibly shown in Fig. 6 and, when converted to stress–strain, shows much more clearly the elastic region. Using the double lap shear avoids the risk of eccentric loadings distorting the results, as well as avoiding the need for offsets in the testing apparatus that could result in slip during the test, at the expense of being more complex to produce the samples and using more material.

When determining the best method for creating a strong joint, the first priority is usually to create a joint with a large maximum load at failure. The joint failing due to the parent material is often the best indicator of a strong joint. However, the elongation at failure is also important, especially for applications subjected to crash loading. A joint with a high elongation has more energy absorption before failure than one with the same failure load but a lower elongation. Further work to aid in this process may be to create functionally graded adhesives or create a process to aid in the use of superwood as a functionally graded adherend to improve the failure by controlling the porosity of the superwood during densification[27].

4.2 Bonding mechanisms

Wood is a naturally porous material, with channels throughout the structure that carried water and nutrients throughout the tree when it was living. The superwood densification process collapses most of these, but the ability of the adhesive to penetrate the surface and create bonds within the superwood still affects the adhesive bonding process. To form a good bond, the adhesive has to penetrate at least two to six cells deep to create a mechanical interlock. The densification makes this more difficult. Natural wood joints strengthen with density, but denser woods make it more difficult to create these strong bonds as there are fewer pathways for the adhesive to penetrate the wood. The way to assist in this is increasing the surface wettability and using pressure during the curing process. The surface damage created during the polishing process can create a larger surface area for the adhesive to apply to, and it also increases the wettability of the surface. The wettability test for natural wood and treated wood such as superwood generally follows that if a piece of wood can have a drop of water spread out and absorb into the wood in 20 s, then that wood will easily form adhesive joints. If it spreads but does not absorb within 40 s, it has good wettability, but not good penetration [9]. Using the wettability test, it was shown that the superwood with no surface treatment had poor wettability, with the samples with random scratches along the surface had good wettability without good penetration when testing using water. The preparation serves to both increase the wettability to aid in adhesive flow across the surface and to open up pores so the pressure applied can help mitigate the poor penetration.

Using pressure during the adhesive process both spreads the adhesive across the surface and forces the adhesive into the pores that remain open. It can also force the adhesive into areas where loose fibers at the superwood surface have created air pockets, displacing the air and filling the area with adhesive. For dense woods, it is recommended in traditional wood joinery to use a force of at least 1.7 MPa, which falls between the two loads used for the superwood samples. This creates the mechanical interlocking through the cells as seen in Fig. 1, while allowing for more contact area between the MMA and cellulose fibers to create hydrogen/chemical bonds.

The issues seen in the patterned superwood could be due to the fracturing it creates within the superwood. Large damage to the surface breaks the superwood and creates weak spots within the bulk around where damage

occurred. These weaknesses then become a point of failure. The dents created during patterning become crack initiators which outstrips their usefulness in allowing the adhesive to penetrate deeper into the superwood. The samples where only the aluminum is patterned while the superwood is scratched give the best of both methods. Patterning the aluminum slightly increases the surface area for the adhesive bonding without noticeably affecting the aluminum as it is ductile enough to undergo the patterning without cracking, while the scratches on the superwood allow for adhesive penetration into the wood without creating failure points.

Additionally, hydrogen bonds play important roles in chemical joint's behavior in wood materials. These bonds form between the functional groups of the adhesive and the hydroxyl groups in the wood cellulose structure [21]. For aluminum alloys, all surfaces are covered by a natural thin layer (typically a few nanometers) of oxide Al_2O_3 [30]. The PMMA adhesive has already been proved to adhere to aluminum oxide (on the surface of aluminum samples) through hydrogen bonds and carboxylate ionic bonding, so the adhesive is known to be suitable for hydrogen bonding adhesion [20]. When the methacrylate polymer reaches the oxide surface of the aluminum, a surface hydroxyl group hydrolyses the ester bond in the side chain of the polymer backbone. As a result of this reaction, a carboxylate anion is formed which bonds ionically with an aluminum cation of the surface [31]. Thus, as shown in Fig. 1, hydrogen/chemical bonding between the Al_2O_3 film on the aluminum surface and MMA adhesive and the cellulose structure in superwood provides the foundational bonds in aluminum-to-superwood joints, in addition to the mechanical interlocks due to adhesive penetration in surface pores/patterns in both superwood and aluminum samples.

It should be pointed out that no direct evidence of chemical bonds has been found between PMMA and superwood, which is a subject of our ongoing research. However, chemical bonds likely play a more dominant role of hydrogen bonds in PMMA/superwood interface, since the shear strength of the joint samples is similar to that of superwood. The superwood material was damaged after the test rather the adhesive itself or adhesive/aluminum interface. This result suggests that the strength of the PMMA adhesive or adhesive/superwood interfacial strength is higher than the chemical bonds between cellulose molecules.

5 Conclusions

Adhesive bonding has been proven an effective joining method for superwood to aluminum alloys in this investigation. The selection of a methacrylate-based adhesive and proper

application (no surface preparation and low force or random orientation polishing and high force) provide high strength (7.5 MPa) for aluminum-to-superwood joints, which is significantly higher (about 50%) than wood-to-wood joints and comparable to aluminum-to-aluminum joints. These results can be improved by patterning the aluminum using a vice and hammer while polishing the superwood with 80 grit sandpaper to create a rougher surface.

The methacrylate-based adhesive bonds to the aluminum (via aluminum oxide film) and superwood through hydrogen bonds. Chemical bonding mechanisms are also likely involved, such as the ionic bonding between aluminum oxide and PMMA, but have not yet been proven between PMMA and superwood. Patterning the aluminum surface allows for more contact area between the adhesive and the aluminum, creating more chances for bonds to form. Surface preparation of the superwood has the same effect on the hydrogen/chemical bonds between cellulose and MMA, while also opening pores in the wood for adhesive to flow into and create a mechanical interlock. Between these, the adhesive is able to bond strongly with both substrates, creating failure in the wood material, whether shallow or deep failure, rather than failure within the adhesive itself.

Declarations

References

1. Song J, Chen C, Zhu S et al (2018) Processing bulk natural wood into a high-performance structural material. Nature 554:224–228. https://doi.org/10.1038/nature25476
2. Barnes T, Pashby I (2000) Joining techniques for aluminum space-frames used in automobiles. J Mater Process Technol 99:62–71. https://doi.org/10.1016/S0924-0136(99)00361-1
3. Lüder S, Härtel S, Binotsch C et al (2014) Influence of the moisture content on flat- clinch connection of wood materials and aluminum. J Mater Process Technol 214:2069–2074. https://doi.org/10.1016/j.jmatprotec.2014.01.010
4. Xie Y, Huang Y, Meng X et al (2020) Friction stir spot welding of aluminum and wood with polymer intermediate layers. Constr Build Mater. 240. https://doi.org/10.1016/j.conbuildmat.2019.117952
5. Yin W, Lu H, Zheng Y et al (2022) Tribological properties of the rotary friction welding of wood. Tribol. Int. 167. https://doi.org/10.1016/j.triboint.2019.105963
6. Rushforth M, Bowen P, McAlpine E et al (2004) The effect of surface pretreatment and moisture on the fatigue performance of adhesively-bonded aluminum. J Mater Process Technol 153–154:359–365. https://doi.org/10.1016/j.jmatprotec.2004.04.319
7. Pereira AM, Ferreira JM, Antunes FV et al (2010) Analysis of manufacturing parameters on the shear strength of aluminum adhesive single-lap joints. J Mater Process Technol 210:610–617. https://doi.org/10.1016/j.jmatprotec.2009.11.006
8. David E, Lazar A (2003) Adhesive bonding between aluminum and polytetrafluoroethylene. J Mater Process Technol 143–144:191–194. https://doi.org/10.1016/S0924-0136(03)00415-1
9. Vick CB (1999) Wood handbook - wood as an engineering material. Madison (Wisconsin): U.S. Dept. of Agriculture, Forest Service, Forest Products Laboratory. Chapter 9, Adhesive Bonding of Wood Materials; p. 9-1-9-24
10. Selbo ML (1975) Adhesive bonding of wood. US Dep Agr Tech Bull 1512:124
11. Ayrilmis N, Candan Z, Akbulut T et al (2010) Effect of sanding on surface properties of medium density fiberboard. Drvna Industrija 61:175–181
12. Özçifçi A, Yapici F (2008) Effects of machining method and grain orientation on the bonding strength of some wood species. J Mater Process Technol 202:353–358. https://doi.org/10.1016/j.jmatprotec.2007.08.043
13. Vitosytė J, Ukvalberginė K, Keturakis G (2012) The effects of surface roughness on adhesion strength of coated ash (Fraxinus excelsior L.) and birch (Betula L.) Wood Mater Sci. 18. https://doi.org/10.5755/j01.ms.18.4.3094
14. Magoss E (2008) General regularities of wood surface roughness. Acta Silv Lign Hung 4:81–93
15. Frihart CR (2005) Adhesive bonding and performance testing of bonded wood products. J ASTM Int 2:12952. https://doi.org/10.1520/STP11654S
16. Pan L, Ding W, Ma W et al (2018) Galvanic corrosion protection and durability of polyaniline-reinforced epoxy adhesive for bond-riveted joints in AA5083/Cf/epoxy laminates. Mater Des 160:1106–1116. https://doi.org/10.1016/j.matdes.2018.10.034
17. Fays S (2003) Adhesive bonding technology in the automotive industry. Adhes Interface 4:37–48
18. Kadioglu F, Es-Souni M (2003) Use of thin adherends in adhesively bonded joints under different loading modes. Sci Technol Weld Join 8(6):437–442. https://doi.org/10.1179/136217103225009080
19. Hu P, Han X, Li WD et al (2013) Research on the static strength performance of adhesive single lap joints subjected to extreme temperature environment for automotive industry. Int J Adhes Adhes 41:119–126. https://doi.org/10.1016/j.ijadhadh.2012.10.010
20. Pletincx S, Marcoen K, Trotochaud L et al (2017) Unravelling the chemical influence of water on PMMA/aluminum oxide hybrid interface in situ. Sci Rep 7:13341. https://doi.org/10.1038/s41598-017-13549-z
21. Gardner DJ, Tajvidi M (2016) Hydrogen bonding in wood-based materials, an update. Wood Fiber Sci 48:234–243
22. Gong M, Lamason C, Li L (2010) Interactive effect of surface densification and post-heat-treatment on aspen wood. J Mater Process Technol 210:293–296. https://doi.org/10.1016/j.jmatprotec.2009.09.013
23. Chinga G, Johnssen PO, Dougherty R et al (2007) Quantification of the 3-D micro-structure of SC surfaces. J Microsc 227:254–265. https://doi.org/10.1111/j.1365-2818.2007.01809.x
24. Schneider CA, Rasband WS, Eliceiri KW (2012) NIH image to ImageJ: 25 years of image analysis. Nat Methods 9:671–675. https://doi.org/10.1038/nmeth.2089
25. Budhe S, Ghumatkar A, Birajdar N et al (2015) Effect of surface roughness using different adherend materials on the adhesive bond strength. Appl Adhes Sci 3(20). https://doi.org/10.1186/s40563-015-0050-4
26. Peng D, Liu Q, Li G et al (2019) Investigation on hybrid joining of aluminum alloy sheets: magnetic pulse weld bonding. Int J Adv Manuf Technol 104:4255–4264. https://doi.org/10.1007/s00170-019-04215-x
27. Khan MF, Sharma G, Dwivedi DK (2015) Weld-bonding of 6061 aluminum alloy. Int J Adv Manuf Technol 78:863–873. https://doi.org/10.1007/s00170-014-6670-1
28. Maćkowiak P, Płaczek D, Sołtysiak A (2019) Mechanical properties of methacrylic plexus MA300 adhesive material determined in tensile test and butt joints of aluminum thick plates. MATEC Web Conf. 290. https://doi.org/10.1051/matecconf/201929001007
29. Dos Reis MQ, Marques EAS et al (2020) Functionally graded adherends in adhesive joints: an overview. Adv Join Process 2:100033. https://doi.org/10.1016/j.jajp.2020.100033
30. Zhu Z, Chen Y, Luo AA et al (2017) First conductive atomic force microscopy investigation on the oxide-film removal mechanism by chloride fluxes in aluminum brazing. Scr Mater 138:12–16. https://doi.org/10.1016/j.scriptamat.2017.05.020
31. Konstadinidis K, Thakkar B et al (1992) Segment level chemistry and chain configuration in the reactive adsorption of poly(methyl methacrylate) on aluminum oxide surfaces. Langmuir 8(5):1307–1317. https://doi.org/10.1021/la00041a012